Available online at www.sciencedirect.com
ScienceDirect
Journal of the European Ceramic Society 29 (2009) 1895–1902
www.elsevier.com/locate/jeurceramsoc

Structure and properties of high Li_2O-containing aluminophosphate glasses

Florian Moreau, Alicia Durán, Francisco Muñoz *

Instituto de Cerámica y Vidrio (CSIC), Kelsen 5, 28049 Madrid, Spain

Received 10 September 2008; received in revised form 9 December 2008; accepted 18 December 2008
Available online 6 February 2009

Abstract

The present study reports on the characterisation of the structure and properties of $50Li_2O{\cdot}xAl_2O_3{\cdot}(50-x)P_2O_5$ glasses. The objective of the work has been to study the influence of the alumina content on the properties of lithium phosphate glasses, and the room temperature ionic conductivity in particular, with potential application as solid electrolytes in lithium secondary batteries. The glass formation domain has been also determined, proving that Al_2O_3 can be introduced only up to 5 mol%. The addition of alumina results in the increase of the glass transition temperature and decrease of the molar volume of the glasses. Furthermore, both chemical durability and room temperature conductivity increase as a function of the alumina content. The structure of the glasses has been followed by means of Fourier-transformed infrared spectroscopy (FTIR) and NMR spectroscopy, which has been used to establish the structure–properties relationship.

Keywords: Glass; Batteries; Ionic conductivity; Chemical properties; Spectroscopy

1. Introduction

Lithium-ion conducting glasses have been widely studied due to their potential application as solid-state amorphous electrolytes in secondary batteries.[1–3] The use of glassy electrolytes in all-solid-state devices may provide numerous advantages, like increased safety, facility of fabrication and miniaturization. At the same time, the amorphous nature of lithium containing glasses allows reaching higher conductivities than those in the crystalline counterpart materials. In particular, phosphate and borophosphate systems were studied by previous authors as candidates for solid electrolytes in lithium-ion secondary batteries.[4,5] Nowadays, glasses and glass-ceramics of the system Li_2S–P_2S_5–P_2O_5 have shown the highest conductivities, which are in the order of 10^{-3} to 10^{-5} S cm^{-1} at room temperature, and best performances as electrolytes in all-solid-state devices.[6,7]

The generally poor chemical durability of phosphate glasses has limited their practical application in real systems. Among the ways to improve the durability of phosphate glasses, the introduction of glass stabilisers represents the most adequate mean. Alkaline-earth, or transition metal ions, as well as intermediate oxides like Al_2O_3 are those which can provide a much higher chemical durability to the phosphate glass. Alumina is particularly known because of its ability to improve the chemical durability of the glasses and reduce their tendency to crystallisation. Previous works proved that alumina can be introduced up to 20 mol% in low alkali containing phosphate glasses.[8] However, only few works are known so far on the properties and structure of high Li_2O-containing aluminophosphate glasses[9–12] and to our knowledge, glasses of the Li_2O–Al_2O_3–P_2O_5 system have not yet been studied for their application as solid electrolytes in rechargeable batteries. The aim of this work has been to study the effect of the addition of Al_2O_3 on the properties of lithium phosphate glasses for a high Li_2O content, i.e. glass transition temperature, molar volume, chemical durability and ionic conductivity. The glass forming ability of the glasses with composition $50Li_2O{\cdot}xAl_2O_3{\cdot}(50-x)P_2O_5$ has been determined and the structure studied by means of nuclear magnetic resonance and Fourier-transformed infrared spectroscopy (FTIR).

2. Experimental

2.1. Glass melting

Lithium aluminophosphate glasses with composition $50Li_2O{\cdot}xAl_2O_3{\cdot}(50-x)P_2O_5$ (x = 0–10), in mol%, have been obtained by conventional melt-quenching procedure. Reagent grade raw materials Li_2CO_3 (Aldrich, 99%) $(NH_4)_2HPO_4$ (Merck, 99%) and $Al(PO_3)_3$ (Aldrich) were weighed and mixed in stoichiometric amounts. The batches were calcined

* Corresponding author.
E-mail address: fmunoz@icv.csic.es (F. Muñoz).

0955-2219/$ – see front matter © 2008 Elsevier Ltd. All rights reserved.
doi:10.1016/j.jeurceramsoc.2008.12.016

in porcelain crucibles up to 450 °C in an electric furnace, then melted for 1 h at temperatures ranging from 800 °C to 1000 °C depending on composition. The melts were poured onto brass plates and annealed slightly above their glass transition temperature. The amorphous nature of all prepared glasses was confirmed by X-ray diffraction (XRD).

2.2. Characterisation of the glasses

Chemical analysis of the glasses was performed through inductively coupled plasma-emission spectrometry (Al_2O_3 and P_2O_5) in a Thermo Jarrel Ash IRIS Advantage equipment and Flame Photometry (Li_2O) in a PerkinElmer 2100 instrument. Prior to the analyses, powdered glass samples were dissolved in diluted hydrochloric acid.

X-ray diffraction analysis of the glasses was carried out with a D-5000 Siemens diffractometer using monochromatic Cu Kα radiation (1.5418 Å).

The thermal expansion coefficient (CTE), the glass transition temperature (T_g) and the dilatometric softening temperature (T_d) were determined from the thermal expansion curve of the glasses obtained in air with a Netzsch Gerätebau dilatometer, model 402 EP, at a heating rate of 5 K min^{-1}. Prismatic samples of around 10 mm in length were used for the measurements and the estimated error on CTE and T_g are ±2% and ±1 K, respectively.

The density of the glasses was measured by helium pycnometry in a *Quantachrome Corp.* multipycnometer by using bulk samples. The molar volume of the glasses (V_m) has been calculated from density measurements by using the equation:

$$V_m(\text{in cm}^{-3}\,\text{mol}^{-1}) = \frac{M}{d} \quad (1)$$

being M the molecular mass, and d the density of the glasses.

The hydrolytic resistance of the glasses was measured in a Soxhlet device at 95 °C, using 100 ml of deionised water of pH 5.5. Prismatic samples of around 8 mm × 5 mm × 3 mm were prepared from annealed glass bars, after polishing with 600 grit SiC paper and cleaned in acetone. The samples were dried at 60 °C until constant weight (±10^{-4} g) and the dissolution rate (D_r) was calculated from the weight loss normalized to the glass surface area and corrosion time.

Electrical conductivity measurements were performed by electrochemical impedance spectroscopy (EIS) in a Gamry REF600 impedance analyser, within the frequency range from 10 Hz to 1 MHz at temperatures between 25 °C and 130 °C, with an applied voltage of 0.5 V. The samples were cut into discs of 1–2 mm in thickness and ∼10 mm in diameter and gold electrodes were sputtered on both faces as contacts for electrical measurements. The electrical conductivity (σ) is determined, for each temperature, through the resistance value (R) read at the low frequency intersection of the semicircle with the x-axis in the Nyquist plots using the sample geometric factor (e/A; e = thickness, A = electrode area) following $\sigma = e/(R{\cdot}A)$ formula. The error in the determination of the conductivity is estimated to be less than 10%.

Fourier transformed infrared spectroscopy of the glasses was performed by using KBr pellets in a *PerkinElmer Spectrum 100* spectrometer in the wave number range of 400–4000 cm^{-1}.

^{31}P MAS NMR spectra were recorded on a Bruker ASX 400 spectrometer operating at 161.96 MHz (9.4 T). The pulse length was 2.5 μs and 60 s delay time was used. A total number of 128 scans were accumulated with a spinning rate of 10 kHz. The ^{31}P spectra were fitted to Gaussian functions, in accordance with the chemical shift distribution of the amorphous state. The precision of the relative component determination was ± 5%. Solid $(NH_4)H_2PO_4$ was used as secondary reference with a chemical shift of 0.82 ppm with respect to H_3PO_4 (85%).

^{27}Al MAS NMR spectra were recorded on a Bruker ASX 400 spectrometer operating at 104.26 MHz (9.4 T). The pulse length was 4 μs and 2 s delay time was used. A total number of 2048 scans were accumulated under a spinning rate of 10 kHz. Solid $Al(SO_4)_2(NH_4){\cdot}12H_2O$ was used as secondary reference with a chemical shift of −0.4 ppm with respect to $Al(NO_3)_3$ 0.1 M.

^{7}Li MAS NMR was performed on Bruker ASX 400 spectrometer operating at 155.51 MHz (9.4 T). The pulse length was 2 μs and 2 s delay time was used. A total number of 256 scans were accumulated under a spinning rate of 10 kHz. Solid LiCl was used as secondary reference with chemical shift of −1.06 with respect to LiCl 1 M solution.

3. Results

3.1. Glass properties

Glass forming interval covered glasses containing up to 5 mol% Al_2O_3. For further additions of alumina, the samples turned opaque during cooling due to crystallisation of undetermined phases. Table 1 gathers the nominal (nom.) and analysed (an.) compositions, in mol%, of the studied aluminophosphate glasses, the glass transition temperature, T_g, the coefficient of thermal expansion (α) measured between 323 K and 573 K, the density and the dissolution rate (D_r) for a corrosion time of 1 h in Soxhlet extractor. The variation of the glass transition temperature and the molar volume (V_m) of the glasses, calculated from density measurements, are plotted in Fig. 1 as a function of the analysed alumina content. T_g increases for increasing alumina content, from 341 °C to 366 °C for 2% and 5% Al_2O_3, respectively, while the molar volume decreases with raise alumina percentage.

Depending on composition, aluminium atoms may be present as different species, i.e. AlO_4, AlO_5 and AlO_6 polyhedra. These new structural units, AlO_n, link phosphate chains giving rise to an increase in the reticulation of the glass network. These stronger O–Al–O bonds compared to the O–Li–O ones, and the possibility of aluminium to behave as network former, are the responsible factors for the observed increase in T_g as well as for the decrease in molar volume of the glasses.

As seen in Table 1, the coefficient of thermal expansion shows only slight changes for the different alumina contents, which can be considered near constant within the limits of error.

Fig. 2 depicts the variation of the Log of dissolution rate (Log D_r) as a function of the analysed alumina content, where D_r is expressed as the weight loss of the glasses by surface area and corrosion time, in g cm^{-2} min^{-1}. Dissolution rate of the

Table 1
Nominal (nom.) and analysed (an.) compositions (in mol%), glass transition temperature, T_g, the coefficient of thermal expansion (α) measured between 323 K and 573 K, density and dissolution rate (D_r) for 1 h corrosion time in Soxhlet extractor of the lithium aluminophosphate glasses.

Glass	Li_2O		Al_2O_3		P_2O_5		T_g ($\pm 1\,^\circ C$)	$\alpha_{323-573\,K}$ ($\times 10^6\,K^{-1}$)	Density ($\pm 0.01\,g\,cm^{-3}$)	D_r ($\times 10^4\,g\,cm^2\,min^{-1}$)
	nom.	an.	nom.	an.	nom.	an.				
50Li2Al	50	49.02	2	2.07	48	48.91	341	17.4	2.38	14.1
50Li3Al	50	49.44	3	3.02	47	47.53	348	16.8	2.40	5.7
50Li4Al	50	49.91	4	3.96	46	46.13	360	18.5	2.41	4.0
50Li5Al	50	49.23	5	5.15	45	45.62	366	17.1	2.42	0.9

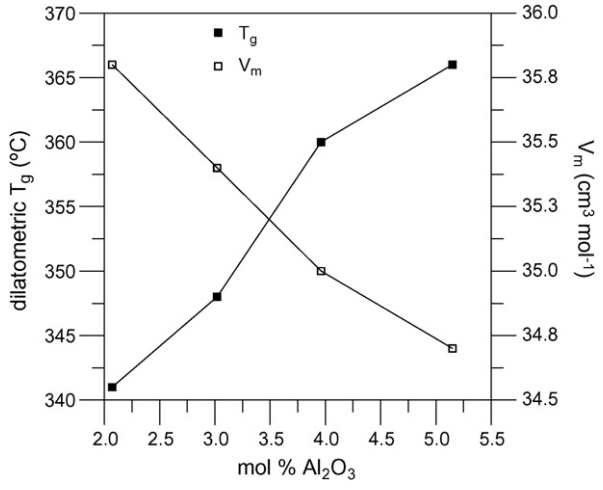

Fig. 1. Variation of the glass transition temperature and the molar volume of the glasses $50Li_2O{\cdot}xAl_2O_3{\cdot}(50-x)P_2O_5$ as a function of the alumina content. Lines are drawn as a guide for the eyes.

$LiPO_3$ glass has been also determined, whose value is included in Fig. 2, though the lithium metaphosphate glass completely dissolved within 15 min corrosion experiment. Log D_r presents an approximately linear decreasing with the alumina content in the studied experimental conditions.

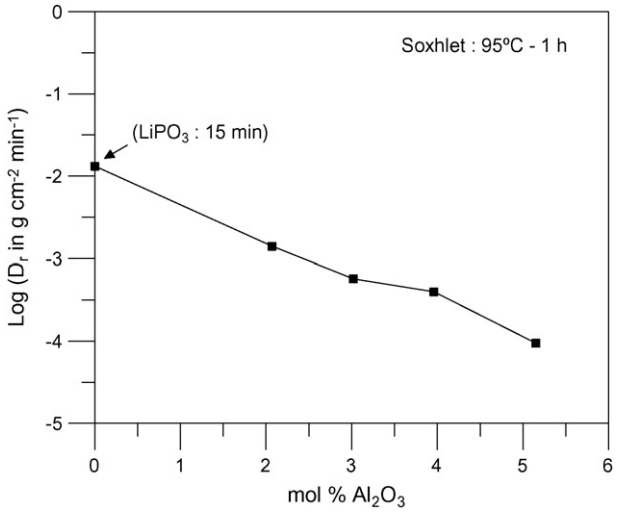

Fig. 2. Log of dissolution rate (D_r), determined from the weight loss in Soxhlet at 95 °C and normalised to the sample surface area and time (in $g\,cm^{-2}\,min^{-1}$), as a function of the alumina content. Line is drawn as a guide for the eyes.

Fig. 3 depicts the Logarithm of the electrical conductivity, Log σ, as a function of the reciprocal absolute temperature for the $50Li_2O{\cdot}xAl_2O_3{\cdot}(50-x)P_2O_5$ glasses. The experimental data follow, within the temperature range studied, the Arrhenius law of the type:

$$\sigma = \sigma_0 \exp\left(\frac{-E_a}{kT}\right) \quad (2)$$

where σ_0 and k are the pre-exponential factor and the Boltzmann constant, respectively, and E_a is the activation energy for conduction. It can be noted from the Arrhenius plots that conductivity increases for increasing alumina contents. In this case, small changes in lithium concentration might also influence ionic conductivity due to the proportionality of the conductivity with the concentration of the charge carriers. Thus, both analysed lithium and aluminium concentrations have been taken into account in order to follow conductivity behaviour of the glasses. The variation of both Log σ at 25 °C, extrapolated from the Arrhenius plots, and the calculated activation energy as a function of the product of analysed contents $[Li_2O][Al_2O_3]$ are

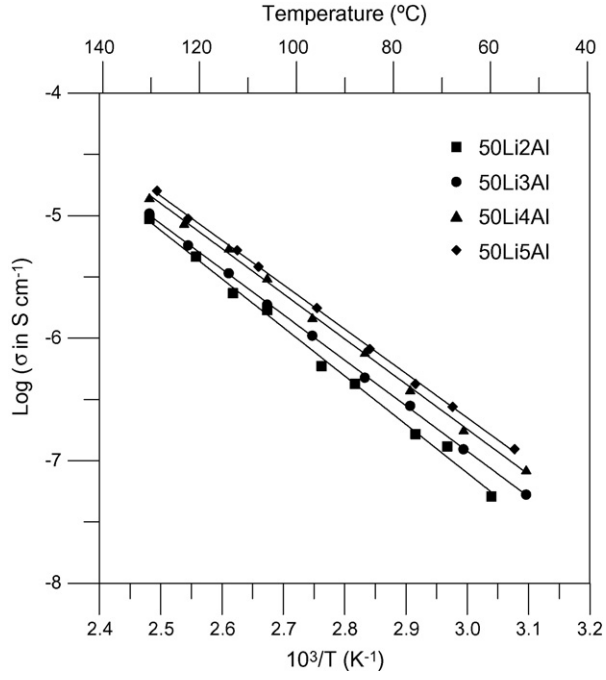

Fig. 3. Arrhenius plots for conductivity of the $50Li_2O{\cdot}xAl_2O_3{\cdot}(50-x)P_2O_5$ ($2 < x < 5$) glasses.

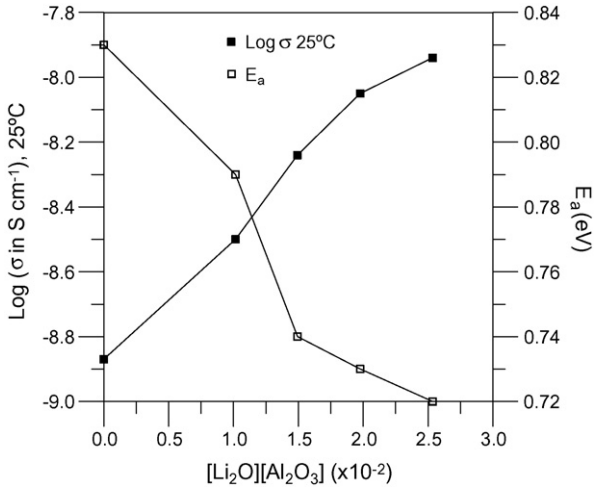

Fig. 4. Logarithm of conductivity, extrapolated at 298 K, and activation energy for conduction as a function of the product of concentrations $[Li_2O][Al_2O_3]$. Lines are drawn as a guide for the eyes.

depicted in Fig. 4. Room temperature conductivity increases for increasing $[Li_2O][Al_2O_3]$, though showing a smaller increasing rate for the highest alumina contents. At the same time, the activation energy for conduction decreases, also in a smaller rate between 3 mol% and 5 mol% Al_2O_3-containing glasses.

3.2. Structural characterisation of the glasses

Fig. 5 shows the FTIR spectra of the $LiPO_3$ and lithium aluminophosphate glasses. All the spectra show characteristic

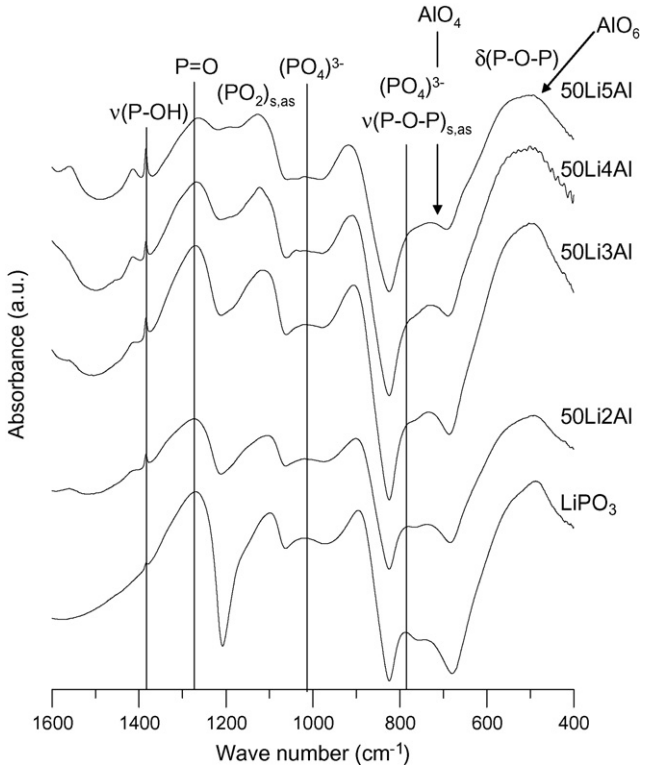

Fig. 5. FTIR spectra of the $50Li_2O{\cdot}xAl_2O_3{\cdot}(50-x)P_2O_5$ glasses.

Table 2
Main vibrations and typical wave numbers of structural groups in phosphate glasses.

Vibrations	Wave number (cm^{-1})
ν(P=O)	1240–1270
ν(P–O–H)	1380
$\nu(P–O–P)_{sym}$	670–800
$\nu(P–O–P)_{asym}$	840–950
δ(P–O–P)	420–620
$\nu(PO_4)^{3-}{}_{sym}$	980–1020
$\nu(PO_4)^{3-}{}_{asym}$	690–800
$\nu(PO_3)^{2-}{}_{sym}$	980–1050
$\nu(PO_3)^{2-}{}_{asym}$	1110–1190
$\nu(PO_2)_{sym}$	1100–1170
$\nu(PO_2)_{asym}$	1200–1300

peaks corresponding to the different vibration modes of the PO_4 tetrahedra as well as those of the P–O–P bonds. Table 2 gathers the main vibrations and their typical wave numbers in phosphate glasses.[13,14] The intensity of the bands corresponding to the P–O–P and PO_4 groups vibrations and, in particular, the one assigned to the PO_2^-, decrease as Al_2O_3 substitutes for P_2O_5 in the glasses. Furthermore, within the range of 400–500 cm^{-1} and 700–800 cm^{-1} new vibrations appear due to the contribution of the sixfold (AlO_6) and fourfold (AlO_4) coordinated aluminium atoms,[13] respectively, though their discrimination with respect to the vibrations assigned to the phosphate groups is not simple to distinguish.

Fig. 6 shows the ^{31}P MAS NMR spectra of the $50Li_2O{\cdot}xAl_2O_3{\cdot}(50-x)P_2O_5$ glasses. All spectra show 3 peaks which are assigned to different resonance bands of the PO_4 tetrahedra as well as PO_4 linked to AlO_n groups. For the 50Li2Al glass, the resonance bands appear at −23 ppm, −11 ppm and −5 ppm. The one at a higher field corresponds to the PO_4 groups of the Q^2-type,[15] with two bringing oxygen atoms bonded to neighbouring phosphorous atoms, typical of the metaphosphate compositions. The band at −5 ppm is attributed to Q^1 groups, either end-chain or pyrophosphate groups, which result from the depolymerisation of the phosphate chains when reducing P_2O_5 content as alumina enters in the glasses. Finally, the resonance band at −11 ppm is attributed to new structural units formed through P–O–Al linkages.[16]

The spectra have been fitted to Gaussian functions with dmfit software [17] and the results of the proportions of phosphate groups and their chemical shifts are given in Table 3. The proportion of the Q^2-type phosphate groups increases with the alumina content. In addition, the amount of the new P–O–Al

Table 3
Relative proportions of the resonance bands attributed to Q^1 and Q^2-type phosphate units and P–O–Al linkages and their respective isotropic chemical shifts (in ppm) in the aluminophosphate glasses for Al_2O_3 contents between 2 mol% and 5 mol%.

Glass	% Q^1	δ Q^1 (ppm)	% POAl	δ POAl (ppm)	% Q^2	δ Q^2 (ppm)
50Li2Al	7.33	−4.78	4.52	−11.45	88.15	−22.63
50Li3Al	8.39	−4.44	5.81	−11.10	85.80	−22.46
50Li4Al	9.21	−4.18	10.14	−10.86	80.65	−22.11
50Li5Al	9.88	−4.06	17.22	−10.74	72.90	−21.42

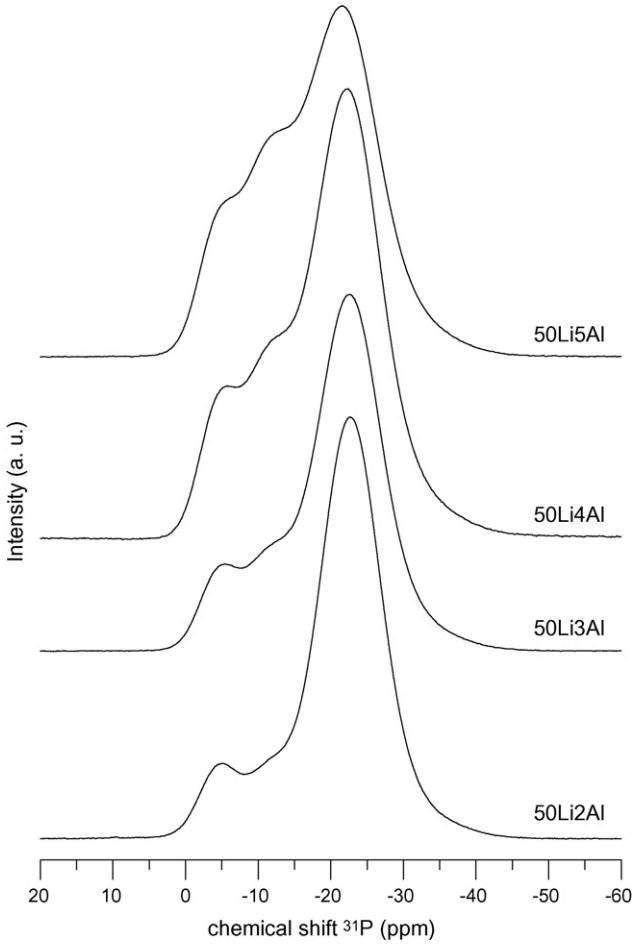

Fig. 6. ^{31}P MAS NMR spectra of the $50Li_2O{\cdot}xAl_2O_3{\cdot}(50-x)P_2O_5$ glasses.

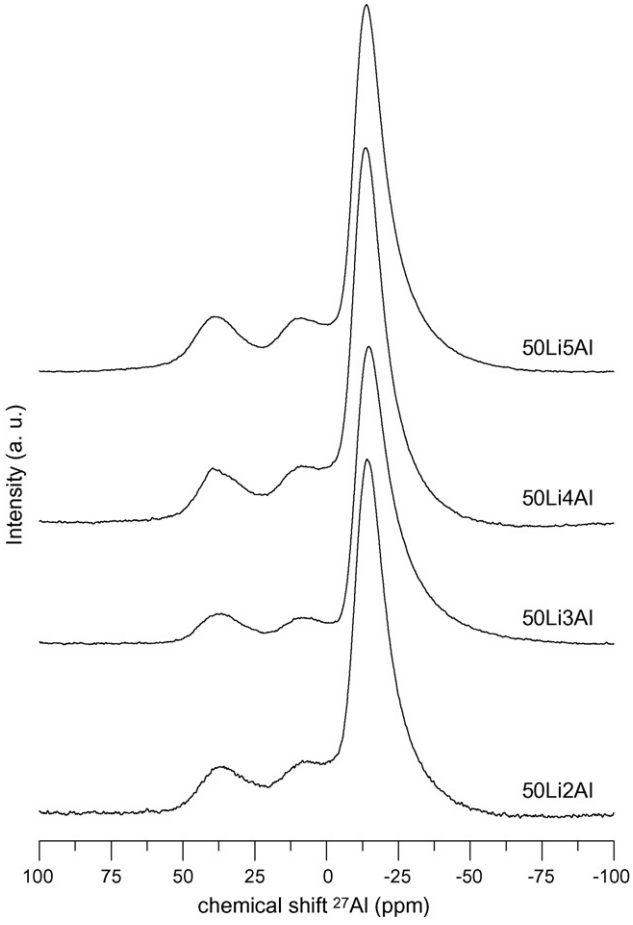

Fig. 7. ^{27}Al MAS NMR spectra of the $50Li_2O{\cdot}xAl_2O_3{\cdot}(50-x)P_2O_5$ glasses.

structural units increases with Al_2O_3, as well as the amount of Q^1 groups though in a lower rate than P–O–Al ones. A small increase in the chemical shift of the three resonance bands can also be observed, which indicates a shortening of the phosphate chains.

Fig. 7 shows the ^{27}Al MAS NMR spectra of the aluminophosphate glasses. Three resonance bands are observed in all the spectra with similar relative proportions independently of the composition. A main resonance band is observed at −13 ppm and attributed to sixfold coordinated aluminium AlO_6. The two smaller ones are assigned to five and fourfold coordinated aluminium at 10 ppm and 37 ppm, respectively.[16] The relative proportions have been estimated by using dmfit[17] with an average error of ±5%, being around 12% for AlO_4 and AlO_5 and 76% for AlO_6, remaining approximately constant within the error limits for all glass compositions.

Fig. 8 depicts the ^{7}Li MAS NMR spectra of the aluminophosphate glasses with 2 mol% and 5 mol% Al_2O_3. They present a single resonance centred at −0.67 ppm, which is characteristic to Li^+ ions with coordination number between 4 and 5, as observed in glasses of the binary system Li_2O–P_2O_5.[18] There is not a significant modification of the position so that no change of the lithium environment can be observed for both alumina contents.

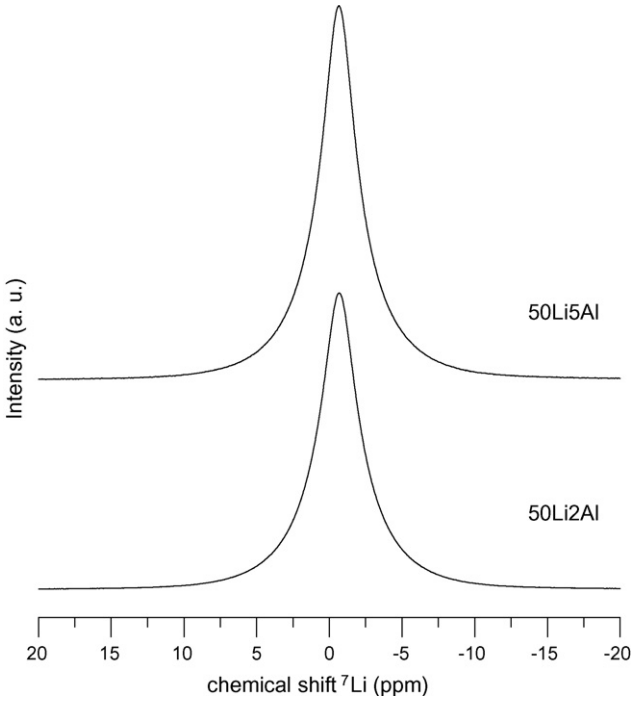

Fig. 8. ^{7}Li MAS NMR spectra of the $50Li_2O{\cdot}2Al_2O_3{\cdot}48P_2O_5$ and $50Li_2O{\cdot}5Al_2O_3{\cdot}45P_2O_5$ glasses.

4. Discussion

4.1. Glass forming ability and structure–properties relationship

According to the results obtained in the present work, it can be pointed out that the higher the Li_2O content, i.e. Li_2O/P_2O_5 ratio, the lower the Al_2O_3 content which is possible to incorporate into the glasses without concurrent crystallisation.

For a metaphosphate glass composition the main structural unit is represented by PO_4 tetrahedron, having two non-bridging and two bridging oxygen atoms, the last joining together adjacent PO_4 groups into a chain-like structure. The addition of alumina in the glass composition is known to form new linkages between the phosphate chains through P–O–Al–O–P bonds. As seen by ^{27}Al NMR (Fig. 7), most of aluminium atoms appear in a sixfold coordination environment and the rest as four- and five-fold coordinated. Previous studies of ^{27}Al NMR in potassium aluminophosphate glasses by Wegner et al.[16] have shown the same behaviour of aluminium polyhedra for low contents of Al_2O_3 as in the lithium aluminophosphate glasses. The proportion of AlO_4 tetrahedra progressively increases with the alumina content in the glasses until being practically the major aluminium species present. An important difference to be pointed out is that in the case of K_2O–Al_2O_3–P_2O_5 glasses, alumina can be incorporated as high as 20 mol%.[16] Therefore, the increase in the alumina content leads to an increase in the "former" character of aluminium atoms. For high Li_2O containing glasses, aluminium behaves mainly like a glass modifier within the range of composition in which it has been possible to obtain totally glassy samples.

The difference between both lithium and potassium aluminophosphate glasses arises from the higher ionic field strength (IFS) of Li^+ ions compared to that of K^+. This is used to explain the lowest tendency of lithium phosphate glasses to incorporate Al_2O_3 as a secondary glass modifier/former. It is known that in glasses of the binary system Li_2O–P_2O_5, the glass forming region accounts for Li_2O contents lower than 60 mol%, otherwise leading to crystallisation of $Li_4P_2O_7$ or Li_3PO_4 phases. On the other hand, in glasses with composition $50Li_2O{\cdot}xB_2O_3{\cdot}(50-x)P_2O_5$, it was observed that $B_2O_3 > 20$ mol% gives rise to crystallisation of lithium orthophosphate.[19] In this work, both lithium and aluminium are assumed to force the development of spontaneous crystallisation for higher Al_2O_3 contents than 5 mol%, when Li_2O is as high as 50 mol%. Moreover, the incorporation of alumina produces not only new P–O–Al–O–P linkages but also gives rise to an increase in the amount of Q^1 groups, indicating a parallel depolymerisation of the phosphate glass network. The behaviour of aluminium atoms as glass modifier will mainly require a higher coordination degree of aluminium than boron atoms, thus leading to a relatively higher depolymerisation degree of the phosphate chains. This difference in the behaviour of boron and aluminium coordination is assumed to be another reason for explaining the lowest tendency of lithium phosphate systems to incorporate alumina avoiding crystallisation.

The modification of the glass structure by the addition of alumina produces a more reticulated and stiff network. The new aluminium polyhedra will form stronger bonds between the phosphate chains through P–O–Al–O–P linkages, giving rise at the same time to a decrease in the free volume of the chain-like phosphate structure of the glass, as well as an increase in the glass transition temperature. The dissolution of phosphate glasses in aqueous medium usually takes place through the hydration and releasing of the phosphate chains into the solution.[20] The increase in the chemical durability of phosphate glasses by addition of alumina is well known.[21] Again, the increased reticulation of the glass network through new P–O–Al–O–P bonds results in a significant improvement of the properties of the glasses and the dissolution of the phosphate chains is now hindered due to the new connections established throughout neighbouring phosphate chains. A change in the mechanism of dissolution of the phosphate glasses is assumed to occur after introduction of Al_2O_3: the increased reticulation, and strength of the P–O–Al–O–P interconnecting linkages, forces the breaking of bonds prior to the dissolution of phosphate groupings after hydration.

4.2. Room temperature conductivity

Different factors might be pointed out as responsible for the increase in the electrical conductivity of the lithium phosphate glasses with alumina additions. As introduced above, aluminium may appear forming three kinds of polyhedra, i.e. AlO_4, AlO_5 and AlO_6, depending on its behaviour as a glass former or glass modifier. The aluminium coordination polyhedra will posses an excess of negative charge, so that lithium ions will be forming charge compensation pairs, with weaker bond strengths than in a typical configuration of modifier cations P–O···Li. The same effect has also been observed in lithium borophosphate glasses when B_2O_3 content increases for a constant 50 mol% Li_2O.[19]

The decrease in the molar volume of the glasses with the alumina content might contribute to the conductivity in two different ways. On the one hand, it would result into an increase in Log σ by reducing the average distance between hopping positions for Li^+ ions. On the other hand, it could act hindering Li^+ migration due to the reduced interstitial volume available. Among these two effects, it is assumed that the one contributing to the increase in conductivity after alumina addition will play a major role, not only because the hopping positions can reduce the distance between each other but also because the incorporation of alumina creates an important number of new hopping positions for Li^+ ions through negatively charged $[AlO_6]$ polyhedra. As observed in Table 3, the amount of Q^1-type phosphate groups increases slightly but, at the same time, P–O–Al new structural units increase from 4 to 17% for Al_2O_3 contents of 2 and 5 mol%, respectively. Then, it is thought that the $[AlO_6]$ polyhedra may act as new conduction paths which will reinforce conduction in Al_2O_3-containing glasses instead of inhibiting charge movement.

The study of the glasses prepared in this study will allow continuing with the development of novel solid electrolytes to

be used in lithium secondary batteries. Another way which has demonstrated to be suitable for increasing the ionic conductivity is the introduction of nitrogen into the phosphate glasses. Thus, LiPON amorphous electrolyte, with a conductivity of around 2×10^{-6} S cm^{-1} at 25 °C, has already been successfully used in microbatteries[4] and an interpretation of the nitrogen influence on the conductivity of oxynitride glasses belonging to the system Li_2O–P_2O_5 was recently published by the authors.[22] In the present case, it has been proved that very low alumina additions improve significantly the transport properties of the glasses, i.e. ionic conductivity and chemical durability, without producing a big change in the glass transition temperature or the coefficient of thermal expansion. The change in conductivity between the lithium metaphosphate glass and the 5 mol% Al_2O_3-containing one is approximately one order of magnitude.

Previous works on the influence of B_2O_3 additions in lithium phosphate glasses with application as solid electrolytes for battery systems, have shown an important improvement of the room temperature conductivity after boron addition.[19] However, for small additions of either B_2O_3 or Al_2O_3, up to 5 mol%, a higher increase in the conductivity of the lithium phosphate glasses is obtained by means of alumina additions instead of B_2O_3. The Log $\sigma_{25\,^\circ C}$ of the glass with composition $50Li_2O{\cdot}5B_2O_3{\cdot}45P_2O_5$ is -8.3 S cm^{-1} while the one found in $50Li_2O{\cdot}5Al_2O_3{\cdot}45P_2O_5$ glass is of -7.9 S cm^{-1}. These results demonstrate that the proper modification of both composition and structure of the lithium phosphate glasses should thus allow the preparation of high Li_2O containing phosphate glasses with high enough ionic conductivity for their application as solid electrolytes. Further research works are currently being performed in the search for new electrolyte materials through the combination of different glass formers or network stabilisers, e.g. alumina, and the processing of their oxynitride counterparts.

5. Conclusions

The properties and structure of high lithium-containing aluminophosphate glasses with composition $50Li_2O{\cdot}xAl_2O_3{\cdot}(50-x)P_2O_5$ were studied to determine the structure–properties relationship. The maximum amount of Al_2O_3 introduced was 5 mol% since further additions gave rise to spontaneous crystallisation. The high Li_2O content, which is necessary for obtaining glasses with a high ionic conductivity, does not allow the introduction of a big amount of alumina when compared with other modifier oxides in aluminophosphate glasses. The addition of alumina to the glass composition produces an increase in the glass transition temperature, the chemical durability of the glasses and in the room temperature conductivity as well. Three kinds of aluminium polyhedra appear, i.e. AlO_4, AlO_5 and AlO_6, being the sixfold coordinated aluminium the most important one, ca. 75%. This groups form also P–O–Al–O–P bonds, thus introducing new linkages between the phosphate chains and increasing the reticulation of the glass network. The increased reticulation of the glass network, together with the formation of negatively charged aluminium polyhedra which act as charge compensating pairs of Li^+ ions, gives rise to a notable increase of the transport properties of the glasses, i.e. chemical durability and ionic conductivity.

Acknowledgements

The authors thank financial funding from the *ENERVID* project (CICYT-MAT2006-4375) of the Spanish National Materials Programme. F. Muñoz acknowledges the I3P contract from CSIC and the authors are also grateful to J.M. Pérez (ICV-CSIC) and M.J. Mata (SIDI-UAM) for the FTIR and NMR characterisation, respectively.

References

1. Minami, T., Hayashi, A. and Tatsumisago, M., Preparation and characterisation of lithium-ion conducting oxysulfide glasses. *Solid State Ionics*, 2000, 1015–1023, 136&137.
2. Cho, K. I., Lee, S. H., Cho, K. H., Shin, D. W. and Sun, Y. K., *J. Power Sources*, 2006, **163**, 223–228.
3. Lee, Y.-I., Lee, J.-H., Hong, S.-H. and Park, Y., Li-ion conductivity in Li_2O–B_2O_3–V_2O_5 glass system. *Solid State Ionics*, 2004, **175**, 687–690.
4. Yu, X., Bates, J. B., Jellison Jr., G. E. and Hart, F. X., A stable thin-film lithium electrolyte: lithium phosphorous oxynitride. *J. Electrochem. Soc.*, 1997, **144**(2), 524–532.
5. Lee, S., Kim, J. and Shin, D., Modification of network structure induced by glass former composition and its correlation to the conductivity in lithium borophosphate glass for solid-state electrolytes. *Solid State Ionics*, 2007, **178**, 375–379.
6. Tatsumisago, M. and Hayashi, A., *J. Non-Cryst. Solids*, 2007, **354**, 1411–1417.
7. Minami, K., Mizuno, F., Hayashi, A. and Tatsumisago, M., *J. Non-Cryst. Solids*, 2008, **354**, 370–373.
8. Metwalli, E. and Brow, R. K., Modifier effects on the properties and structure of aluminophosphate glasses. *J. Non-Cryst. Solids*, 2001, **289**, 113–122.
9. Gur'ev, N. V. and Pronkin, A. A., Mixed-alkali effect in aluminophosphate glasses. *Glass Phys. Chem.*, 1983, **9**, 258–260.
10. Jurado-Egea, J. R. and Fernández-Arroyo, G., Etude de comportement électrothermique de verres, dans les zones de transformation structural. *J. Non-Cryst. Solids*, 1980, 335–340, 38&39.
11. Faivre, A., Viviani, D. and Phalippou, J., Mixed-alkali effect in Li and Na aluminophosphate glasses: influence of the cation environment. *Solid State Ionics*, 2005, **176**, 325–332.
12. Isard, J. O. and Mallick, K. K., Analysis of the lithium ion conductivity in aluminium metaphosphate glasses. *Solid State Ionics*, 1986, **21**, 7–18.
13. Belkébir, A., Rocha, J., Esculcas, A. P., Berthet, P., Gilbert, B., Gabelica, Z. *et al.*, Structural characterisation of glassy phases in the system Na_2O–Al_2O_3–P_2O_5 by MAS and solution NMR EXAFS and vibrational spectroscopy. *Spectrochim. Acta A*, 1999, **55**, 1323–1336.
14. Elisa, M., Cristina Vasiliu, I., Grigorescu Cristina, E. A., Grigoras, B., Niciu, H., Niciu, D. *et al.*, Optical and structural investigation on rare-earth-doped aluminophosphate glasses. *Opt. Mater.*, 2006, **28**, 621–625.
15. Lippmaa, E., Magi, M., Samoson, A., Engelhardt, G. and Grimmer, A. R., Structural studies of silicates by solid state high resolution ^{29}Si NMR. *J. Am. Chem. Soc.*, 1980, **102**, 4889–4893.
16. Wegner, S., Van Wullen, L. and Tricot, G., The stucture of aluminophosphate glasses revisited: Application of modern solid-state NMR strategies to determinate structural motifs on intermediate length scales. *J. Non-Cryst. Solids*, 2008, **354**, 1703–1714.
17. Massiot, D., Fayon, F., Capron, M., King, I., Le Calvé, S., Alonso, B. *et al.*, Modelling one- and two-dimensional solid state NMR spectra. *Magn. Reson. Chem.*, 2002, **40**, 70–76.

18. Alam, T. M., Conzone, S., Brow, R. K. and Boyle, T. J., *J. Non-Cryst. Solids*, 1999, **258**, 140–154.
19. Muñoz, F., Montagne, L., Pascual, L., and Durán, A., Composition and structure effects on the properties of lithium borophosphate glasses showing boron anomaly. *J. Non-Cryst. Solids*, submitted for publication.
20. Vogel, W., in *Glass Chemistry*, 2nd Edition, 1994, 164–165.
21. Bunker, B. C., Arnold, G. W. and Wilder, J. A., Phosphate glass dissolution in aqueous solutions. *J. Non-Cryst. Solids*, 1984, **64**, 291–316.
22. Muñoz, F., Durán, A., Pascual, L., Montagne, L., Revel, B. and Rodrigues, A. C. M., Increased electrical conductivity of LiPON glasses produced by ammonolysis. *Solid State Ionics*, 2008, **179**, 574–579.